



Small Modular Reactor based on NuScale with Thorium base

Gonçalves ^{a*}, D.M.E., Silva^a, M.V.; da Cunha ^b, C. J. C.M.R.; Stefanni^a, G. L.

^a Nuclear Engineering Program / Universidade Federal do Rio de Janeiro / COPPE, Av. Horácio Macedo, 2030, Bloco G - Sala 206 - CT, University City, Rio de Janeiro, RJ, Brazil

^b Centro Regional de Ciências Nucleares do Nordeste (CRCN-NE/CNEN), Av. Prof. Luis Freire N°200- Curado, Recife - PE, 50740-437, Brazil

*Correspondence: diegomanoelgoncalves@gmail.com ; cjcuncunha@gmail.com

Abstract: This study proposes a novel approach to enhance the NuScale Small Modular Reactor (SMR) by incorporating mixed uranium-thorium (U-Th) oxide fuel, thereby increasing U-233 production, improving fuel use, and reducing radioactive waste. The research integrates advanced neutron transport simulations with optimization techniques to refine the reactor's fuel design for greater sustainability and efficiency. The researchers modeled the reference NuScale reactor core using the SERPENT code, which relies on the Monte Carlo Method (MCM) to ensure exact neutron transport simulations. To meet substantial computational demands, they ran these simulations on the Lobo Carneiro supercomputer at NACAD/UFRJ. The team applied a Particle Swarm Optimization (PSO) algorithm to find the best seed-to-blanket volume ratio, thereby maximizing U-233 production and achieving a self-sustaining fuel cycle. Implemented in Python, the algorithm continuously adjusted reactor parameters, logged progress, and enabled ongoing monitoring and potential restarts. For the seed region, the researchers employed a 13x13 configuration and used a 19x19 configuration for the blanket. They evaluated the proposed core design against critical safety and performance metrics, including the Moderator Temperature Coefficient (MTC), Doppler Temperature Coefficient (DTC), boron worth coefficient (BWC). The team also conducted data analysis and visualization using *SerpentTools* in Python. The results show that integrating U-Th fuel into SMRs can boost reactor performance without compromising safety, thereby offering a promising path toward more sustainable, efficient, and scalable nuclear energy production. This approach can reshape next-generation nuclear reactors by addressing essential challenges related to fuel sustainability and waste management.

Keywords: Reactor Core; Fuel Cycle; NuScale, SMR, Nuclear fuel cycles.



Pequeno Reator Modular Baseado em NuScale com Base de Tório

Resumo: Este artigo propõe avaliar o conceito de elemento combustível, proposto por Radkwosky, que apresenta uma composição heterogênea com duas regiões distintas: uma região fértil no exterior e uma região físsil no interior. O conceito foi analisado comparando dados do núcleo convencional modelado com o código SERPENT. Os resultados obtidos foram utilizados para projetar um núcleo completo, com o objetivo de avaliar o desempenho, segurança e compará-lo com o núcleo original do Pequeno Reator Modular (SMR) da NuScale, atualmente em fase final de licenciamento. A análise da queima de combustíveis é fundamental para garantir um equilíbrio na queima dentro do núcleo, ajustar o coeficiente de reatividade, e gerenciar a queima de boro e outros venenos queimáveis, elementos cruciais para a segurança nuclear e a redução de resíduos de combustível. Foi verificado que é possível integrar esse novo conceito ao núcleo do PRM sem comprometer significativamente a segurança do reator. O estudo inclui diversas simulações computacionais, neutrônicas e termo-hidráulicas, fundamentais para validar a viabilidade e confiabilidade técnica deste novo conceito de combustível, oferecendo uma opção mais flexível e segura para a produção de energia nuclear em grande escala.

Palavras-chave: Núcleo do reator; Ciclo do combustível; NuScale, SMR, ciclos de combustível nuclear.

1. INTRODUCTION

The global pursuit of more sustainable and efficient energy solutions has become a driving force in mitigating the environmental impacts associated with traditional energy generation methods. In this context, despite their significant advantages, the expansion of nuclear energy still faces economic challenges, concerns about proliferation, safety, and waste management. A promising alternative to overcome these obstacles is the adoption of small modular reactors (SMRs). These compact reactors, with thermal power outputs ranging from 50 MW to 200 MW, are factory-built and offer advantages over conventional reactors, including modular construction, scalability, extended fuel cycles, passive safety systems, and reduced costs (Black et al., 2021).

Among the pioneering companies in SMR development is NuScale, whose reactor design is particularly suited for both electricity cogeneration and water desalination. This feature is crucial in regions with scarce water resources and limited electrical infrastructure (Ingersoll, 2014; 2021). The NuScale design, classified as an advanced Generation III+ light water reactor (LWR), was conceived to address economic challenges, enhance safety, and reduce nuclear waste proliferation. These qualities make SMRs attractive in areas with restricted energy storage ability or difficult access, standing out for their high availability, reliability, and passive cooling systems associated with a compact core.

The choice of the NuScale design in this study is justified by the lower initial investment—approximately 61% less than that of a conventional plant of the same capacity—and by the lower level of risk, evidenced by the higher net present value relative to net debt. This more favorable risk–return ratio (Black et al., 2021) drives interest from investors and policymakers, although the widespread adoption of SMRs depends on stakeholders' willingness to accept their costs and risks. Consequently, the existence of a

robust regulatory framework and an infrastructure capable of integrating the technology with other renewable sources becomes imperative, overcoming the impasse outlined by Locatelli et al. (2014) and Black et al. (2021).

This work aims to convert NuScale's SMR for the use of thorium-based (U,Th)O₂ fuel. Owing to the reactor's operational and design characteristics, such a conversion may reduce the risk of nuclear weapons proliferation, improve waste management, and lower total construction and storage costs compared with an open-cycle UO₂ reactor. The Seed-Blanket (SB) concept, proposed by Radkowsky (1985) and later studied by Radkowsky (1985), Stefani et al. (2023), Silva et al. (2024), and Gonçalves et al. (2024), involves dividing the reactor core into two regions—one having fissile elements (seed) and the other containing fertile elements (blanket). This approach makes it possible to optimize the neutron spectrum, maximizing ²³³U production in the fertile region while minimizing ²³⁹Pu generation in the fissile region.

Thorium appears as a promising alternative to uranium due to several physical and economic advantages. Although it is more abundant, only a fraction is economically exploitable. Even so, thorium-based reactors can produce smaller amounts of long-lived waste and reduce actinide production, helping waste management. Furthermore, thorium is converted into ²³³U, a stable and efficient fuel, thereby improving burnup and reducing overall fuel consumption. This technology can be applied in various reactor types—light water reactors (LWRs), heavy water reactors (HWRs), and high-temperature gas-cooled reactors (HTGRs)—and is particularly attractive to countries with large thorium reserves, such as Brazil and India (C.A. Lobo & Stefani, 2024).

To address the challenges of design and operational optimization for these systems, the application of particle swarm optimization (PSO) algorithms, developed by Kennedy (1995), is promising. PSO has been successfully employed in a wide range of problems, including energy system planning and control (AlRashidi, 2010), and it has been applied

in the nuclear reactor context geometry and part layouts—such as fuel assemblies and control rods—aiming for improvements in system efficiency and safety (AlRashidi, 2009; 2010). For instance, Xu (2021) proved the use of nonlinear dissipative particle swarm algorithms for core design optimization, resulting in enhanced safety and performance. Similarly, Khorasani (2018) applied PSO to control rod positioning in nuclear reactors, achieving gains in power generation and reductions in operational costs.

2. METHODOLOGY

The procedure for converting the NuScale small modular reactor to use a uranium–thorium oxide (U–Th) mixture aimed to increase the production of U-233 and enhance resource use. To achieve this primary objective, the following secondary objectives were pursued: modeling a reference NuScale reactor to ensure the reliability of the model; conducting a particle swarm optimization (PSO) study on a single fuel assembly to define the optimal seed and blanket volume, so as to maximize conversion and maintain a self-sustaining reaction; and using the dimensional parameters obtained from this study to define the full core and compare the results with a standard core.

In the first phase of the study, it was necessary to reconstruct the SMR–NuScale reference core in the SERPENT code, which uses the Monte Carlo Method (MCM) to solve the transport equation. To ensure the accuracy of the results, the Lobo Carneiro supercomputer at NACAD/UFRJ was used, given its high processing capacity. The same design parameters described by Valtavirta (2023) were employed, including a population of 100,000 neutrons, with 1,000 active cycles and 100 inactive cycles.

In parallel, a Particle Swarm Optimization (PSO) algorithm, according to Kennedy (1995), AlRashidi (2009), Tong et al. (2023), and Xu (2021), was implemented in Python to run sequentially. PSO optimizes a fitness function by iteratively adjusting

the positions and velocities of the particles based on the best individual and collective solutions, with functionalities for particle initialization and sequential fitness function evaluation. Next, the fuel assembly configuration was obtained using both PSO (Silva et al., 2024) and a parametric approach (Gonçalves et al., 2024), varying only the moderator-to-fuel volume ratio while keeping a 13×13 configuration for the seed region and 19×19 for the blanket region.

The results of the generations are recorded in a file, and the optimization process state can be retrieved, easing restart or progress monitoring. This sequential approach was chosen to automate the algorithm, thereby reducing workload; the processing was performed on a cluster at the Laboratory of Monitoring and Processes (LMP).

Moreover, this study aims to analyze and compare the cores of two different nuclear reactors with respect to critical parameters such as the Moderator Temperature Coefficient (MTC), the Doppler Temperature Coefficient (DTC), Boron Worth Concentration. The outputs will be collected and processed in Python via the SerpenTools package (Andrew Johnson, 2020). The method described below details the necessary steps for conducting this comparative analysis, providing a comprehensive overview of the variations between the two nuclear models.

2.1. Particle Swarm Optimization (PSO)

This section presents the method based on the Particle Swarm Optimization (PSO) algorithm, a biologically inspired technique that simulates the behavior of animals in search of resources such as food or shelter. In computational terms, each animal is modeled as a particle that is a potential solution within the search space. The particles interact with one another, adjusting their positions and velocities according to the history of their own best positions and the best global position found by the swarm.

The equations provided describe the basic functioning of the PSO algorithm in the search for best solutions, as well as the fitness function used to assess the quality of those

solutions. The velocity of each particle in the swarm, at iteration $(t+1)$, is updated from its current velocity, taking into account the best point previously found by the particle itself ($pbest$) and the best point found by the swarm ($gbest$). The formula is:

$$v(t+1) = w \cdot v(t) + c1 \cdot r1(t) \cdot (pbest(t) - x(t)) + c2 \cdot r2(t) \cdot (gbest(t) - x(t)) \quad (1)$$

The particle position is updated based on the new velocity value calculated in the earlier step:

$$x(t+1) = x(t) + v(t+1) \quad (2)$$

After calculating the new velocity, the particle moves to a new position in the search space, which is the sum of its current position and the new velocity. This reflects the “physical” movement of the particle toward regions with higher potential quality, according to information from the swarm.

2.2. Fitness Function:

The fitness function evaluates the quality of each solution found. It is given by, where CR is the resource conversion rate (for example, the efficiency of nuclear fuel use or another parameter related to resource conversion in the reactor), and U^{233} denotes the concentration of the Uranium-233 isotope in the system.

$$f = 10^3 CR + \frac{U^{233}}{10^{-3}} + e^{-K_{\infty}} \quad (3)$$

Therefore, it is ensured that the solutions proposed by the particles are evaluated considering both efficiency (maximizing fuel use) and the safety and operational viability of the reactor (reflected in reactivity).

The describes the iterative cycle of the algorithm coupled to the SERPENT code. First, variable first parameters are defined, chosen randomly within pre-established limits. These values are inserted into the script that generates the input file, starting the

simulation. At the end of the execution, the results obtained are evaluated by a fitness function. Based on this evaluation, a new population of solutions is created, restarting the process. This cycle repeats until a stopping criterion, such as convergence or maximum number of iterations, is reached. At the end, the best solutions obtained are listed.

The table shows the parameters used in the PSO simulation. The optimization problem considered has a dimension of 80, and 100 particles are used in the swarm. The inertia weight (0.729) influences the persistence of the previous velocity of the particles, while the cognitive (2.0) and social (1.8) weights determine the inclination of the particles to search for the best solution for themselves and the swarm, respectively. Finally, the maximum velocity (2.0) limits the magnitude of the displacement at each iteration, controlling the exploration of the search space.

The table 1, outlines the parameters used in the PSO simulation. The optimization problem has a dimensionality of 80, with a swarm size of 100 particles. The inertia weight (0.729) regulates the influence of a particle's earlier velocity, promoting stability and exploration. The cognitive (2.0) and social (1.8) coefficients guide particles toward their personal best positions and the global best position, respectively, balancing individual and collective learning. Lastly, the maximum velocity (2.0) constrains the size of displacement per iteration, ensuring controlled exploration of the search space.

Table 1: Table of parameters PSO.

| Parameters | Value |
|---------------------|-------|
| Number of particles | 100 |
| Inertia weight | 0.729 |
| Cognitive weight | 2.0 |
| Social weight | 1.8 |
| Maximum speed | 2.0 |

2.3. Neutronic parameters and reactivity coefficients

This analysis compared two nuclear reactor cores: a standard NuScale model and a PSO-optimized Seed-Blanket type. Key parameters evaluated were the Moderator Temperature Coefficient (MTC), Doppler Temperature Coefficient (DTC), and Boron Concentration (BWC), using Serpent-Tools. The effective multiplication factor (k_{eff}) was found in the Full Hot Power (HFP) state from SERPENT burnup simulations. Reactivity coefficients were calculated using Python, considering various temperatures and water densities based on IAPWS properties.

2.4. Boron Worth Coefficient (BWC)

Reactivity in nuclear reactors measures the variation in the reaction rate in relation to the criticality condition, and is expressed by equation (4):

$$\rho = \frac{k_{eff} - 1}{k_{eff}} \quad (4)$$

The change in reactivity ($\Delta\rho$) reflects the difference between two reactor states. The Boron Worth Coefficient (BWC) quantifies how reactivity changes with the concentration of boron in the coolant, present as boric acid (H_3BO_3). It is typically expressed in pcm/ppm, where pcm indicates a reactivity change of 1/100,000 and ppm denotes the boron concentration. Mathematically, the BWC is the relationship between reactivity change and boron concentration variation (ΔC_B).

$$\alpha_{BWC} = \frac{\Delta\rho}{\Delta C} \quad (5)$$

2.5. Doppler Temperature Coefficient (DTC).

The Doppler Temperature Coefficient (DTC) quantifies how a nuclear reactor's reactivity responds to changes in fuel temperature. Typically negative, the DTC shows that higher fuel temperatures decrease reactivity. In this analysis, the fuel temperature was

varied in 100 K increments from 600 K to 1800 K, with fuel density recalculated as needed, while the moderator temperature was kept constant at 600 K.

$$\alpha_{DTC} = \frac{\Delta\rho}{\Delta T_f} \quad (6)$$

2.6. Moderator Temperature Coefficient (MTC).

The Moderator Temperature Coefficient (MTC) measures how the reactivity of the reactor varies with the temperature of the moderator, which slows down neutrons to ease nuclear fission. This parameter is essential for assessing the stability of the reactor. The relationship between the change in reactivity ($\Delta\rho$) and the change in moderator temperature (ΔT_m) is given by equation (7):

$$\alpha_{MTC} = \frac{\Delta\rho}{\Delta T_m} \quad (7)$$

In this analysis, the moderator temperature was adjusted in 4 K increments within the range of 494.15 K to 560.15 K. The moderator density was recalculated according to the thermodynamic properties from IAPWS.

2.7. Power Linear

Power density in a nuclear reactor is the amount of power generated per unit length of nuclear fuel, typically expressed in watts per centimeter (W/cm). It is a critical parameter in thermal analysis, as it directly affects the temperature distribution within the reactor core and the efficiency of heat removal by the cooling system. Higher power densities lead to greater temperature gradients. The power density is calculated using equation (8), where it is the power density in W/cm³, r_i is the reaction rate in the cell, P is the total system power in watts, and V_j is the cell volume.

$$p_i = \frac{r_{ij} \times P}{\sum_{j=0}^n r_j \times V_j} \quad (8)$$

The developed code performs a comprehensive analysis of power density in a nuclear reactor using detector data extracted from the SERPENT output file. Its workflow includes file management, extraction of detector coordinates and related data, calculation of cell volumes and areas, and determination of linear power density along various axes. Additionally, the code generates three-dimensional visualizations of power density and linear flux distributions, storing the results for subsequent analysis. The entire process accounts for the three-dimensional grid structure and power parameters specified in the input file, ensuring right and detailed assessments.

2.8. Thermohydraulic analysis.

We adapted the CFD single-channel heated model originally developed by (Cunha, et al., 2024) for the AP1000 reactor core and the AP-Th1000 concept to analyze an internal subchannel of the NuScale and SBU cores. The fuel rod-centered cell subchannel approach, as presented in, was changed to a coolant-centered cell configuration to optimize the computational meshing step. This adaptation allows for a more efficient and robust analysis of the thermal and fluid flow conditions inside the subchannel.

We used Ansys *SpaceClaim* to create a 3D model of the subchannel region of the standard NuScale core and SBU. For the NuScale model, we followed the dimensions and operating conditions specified in the final safety report given to the NRC (NuScale Power, 2020), ensuring adherence to the original design. The geometry was adjusted to accommodate the SBU core, exploiting symmetries to optimize the modeling of both cores, increasing the efficiency of thermal and hydraulic analysis. The discretization was done with Ansys Meshing, generating a mesh with 9.21 million nodes and 8.45 million elements, mainly hexahedral. The materials followed the specifications of (Cunha, et al., 2024), with adjustments in the enrichment of uranium dioxide and replacement of Zircaloy-4 by M5, a variant of the Zr alloy with 1% Nb with a recrystallized microstructure,

in the fuel cladding manufactured by AREVA, according to the AP1000 and NuScale projects (Westinghouse, 2011) (NuScale Power, 2020).

The thermophysical properties of M5 were based on (Kecek, et al., 2016). The k-omega SST turbulence model was used to capture the heat transfer between the fuel rod and the coolant. The boundary conditions included inlet mass flow, outlet pressure, and symmetry on the side faces. The mass flow of the standard NuScale core is 587.15 kg/s, with an inlet temperature of 531.48 K and a pressure of 12.755 MPa (NuScale Power, 2020). We used a sinusoidal approach, as per (Todreas & Kazimi, 2011), for the axial distribution of the power density, applied as volumetric power generation in Ansys CFX. The maximum linear power was obtained with the SERPENT code, ensuring accuracy under the operating conditions of both cores.

3. RESULTS AND DISCUSSIONS

3.1. Core Modeling

Table 2 summarizes the key geometric parameters of the NuScale reactor, including core height, fuel cladding spacing, and part thicknesses. Engineers constructed the reactor vessel using SSA508 steel and incorporated SS304 and SS304L stainless steels for the reflectors, as illustrated in Figure 1.

Table 2: Design parameters NuScale x SBU.

| Parameters | Unit | NuScale | SBU |
|-------------------------|--------|----------|----------|
| Total height | [cm] | 243.5610 | 243.5610 |
| Gap | [cm] | 0.0065 | 0.0065 |
| Cladding thickness | [cm] | 0.0042 | 0.0042 |
| Fissile Fuel radius | [cm] | 0.4058 | 0.2651 |
| Fertile fuel radius | [cm] | - | 0.40521 |
| Numbers of fissile rods | [unid] | 17 | 13 |

| Parameters | Unit | NuScale | SBU |
|----------------------------|--------|-----------|----------|
| Number of Fertile Rods | [unid] | - | 19 |
| Fissile Fuel Pitch | [cm] | 1.2598 | 0.78038 |
| Fertile Fuel Pitch | [cm] | - | 1.13157 |
| Fissile Fuel (Vm/Vf) Ratio | [-] | 2.0680 | 1.75834 |
| Fertile Fuel (Vm/Vf) Ratio | [-] | - | 1.48233 |
| Inner Reflector Diameter | [cm] | 188.5655 | 188.5655 |
| Outer Reflector Diameter | [cm] | 198.72549 | 198.7254 |
| Inner Vessel Diameter | [cm] | 256.50079 | 256.5007 |
| Outer Vessel Diameter | [cm] | 290.9161 | 290.9161 |

To align the SBU core's K_{eff} and CR values with results from the Particle Swarm Optimization (PSO) algorithm, the research team parametrically adjusted and interpolated fuel enrichments. Figure 1 compares two types of NuScale reactor cores: the Standard NuScale core (left) and the NuScale SBU core (right). The Standard NuScale core relies on fuel elements enriched in uranium-235 from 1.50% to 4.55% wt., with some elements having gadolinium to manage reactivity. In contrast, the SBU core uses UO_2 enriched between 17% and 20% wt. combined with $(Th,U)O_2$ blankets ranging from 81% to 96%. This configuration enhances fuel efficiency and fosters the production of U-233 from thorium, resulting in a more sustainable operation.

Figure 1: Loading Pattern (a) NuScale (b) NuScale-SBU.

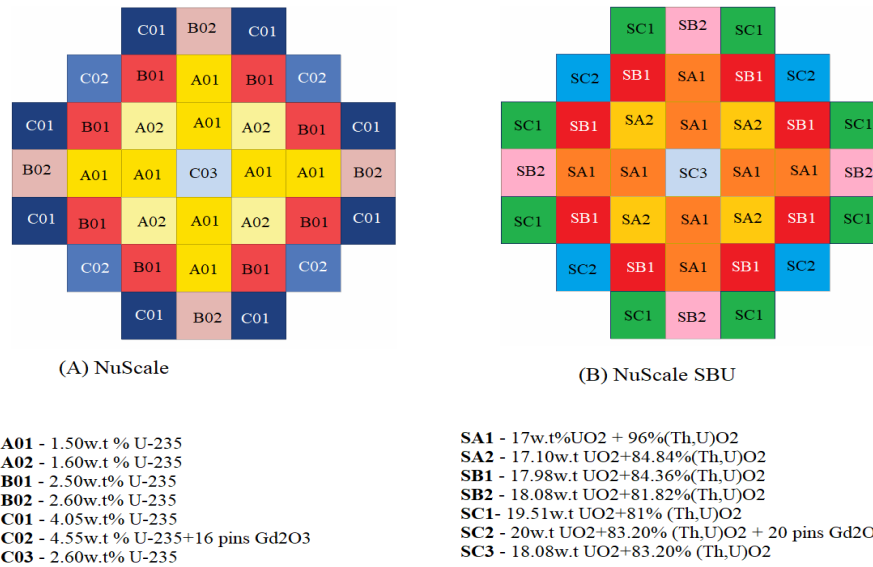
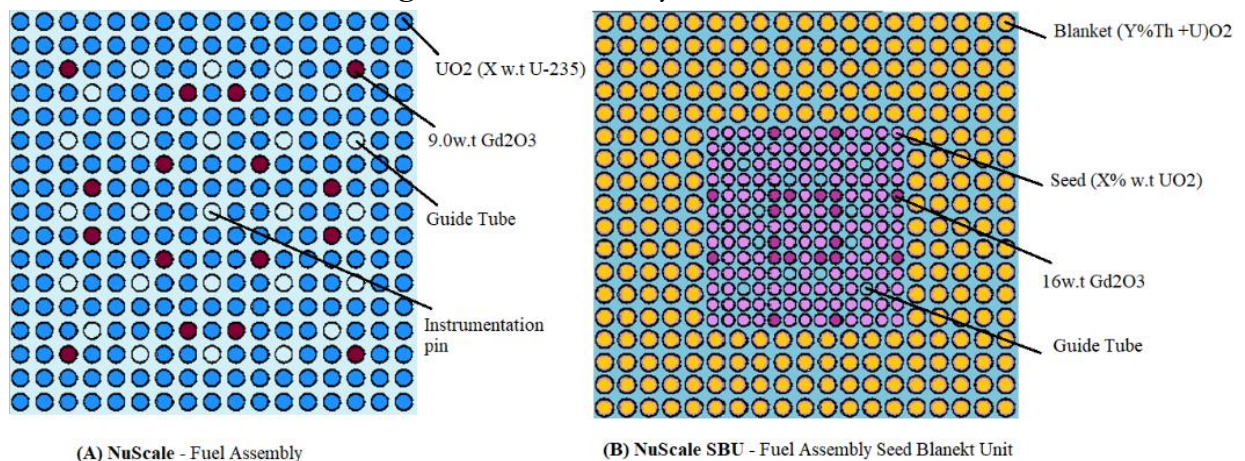


Figure 2 illustrates two fuel assembly configurations employed in nuclear reactors. The assembly on the left features a 17x17 grid composed of UO₂ fuel elements, with select rods enriched with 16 wt.% Gd₂O₃ to regulate reactivity. Guide tubes are strategically positioned to accommodate control rods or instrumentation. The configuration on the right presents a more complex structure, comprising a 19x19 grid with (U,Th)O₂ fuel elements arranged along the periphery and a central 13x13 grid of pure UO₂. Like the first configuration, guide tubes and Gd₂O₃-enriched elements are incorporated to enhance reactivity management.

Figure 2: Fuel assembly NuScale x SBU.



The SERPENT simulation data were evaluated to compare the performance of the proposed reactor model against the standard core configuration. Figure 3 illustrates the variation of the effective multiplication factor (k_{eff}) over an 800-day burnup period in the NuScale (blue) and SBU (orange) reactors. Initially, both reactors run in a supercritical state, with (k_{eff}) values of 1.14447 for NuScale and 1.08138 for SBU. As fuel burnup progresses, neutron production declines until equilibrium is reached. The SBU reactor proves extended operational longevity and reduced waste generation due to a lower production of Xe-135 and a 15.48% higher fuel conversion rate. Both systems eventually stabilize, employing comparable reactivity control strategies.

Figure 3: Comparison of the effective multiplication factor.

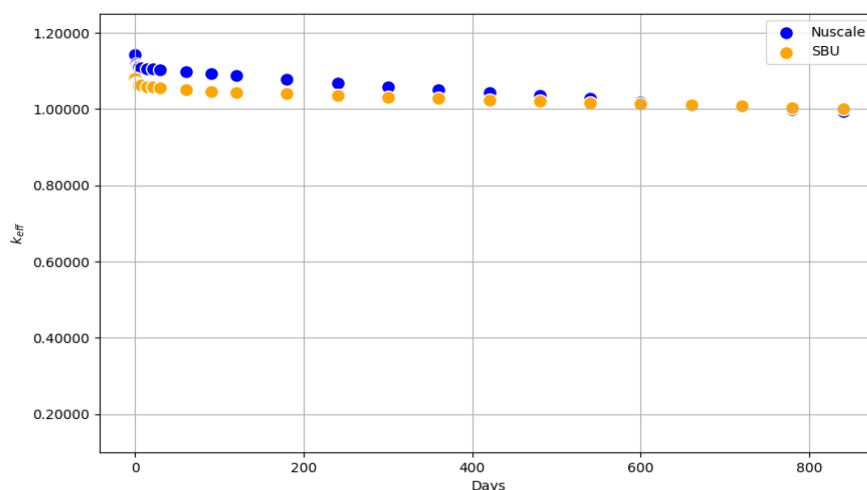


Figure 4 illustrates the comparative analysis of Boron Reactivity Coefficients (BWC) in pcm/ppm for different reactor cores. The graph reveals that the NuScale core (depicted in blue) shows a stable BWC across varying boron concentrations, signifying enhanced neutron absorption efficiency. Conversely, the SBU core (represented in orange) proves a BWC that becomes progressively less negative as boron concentration increases, reduced stability and heightened sensitivity compared to the NuScale core.

Figure 4: Comparison of the value of the boron coefficient (BWC).

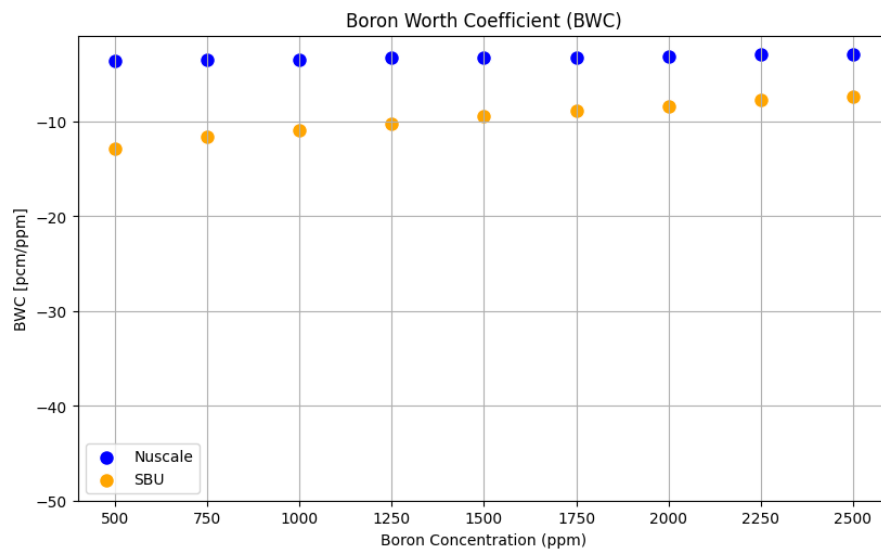
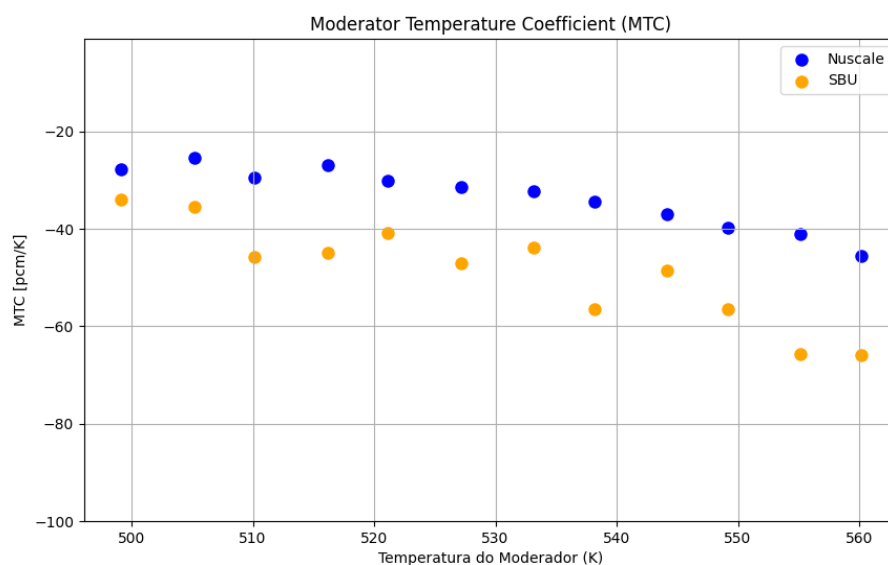


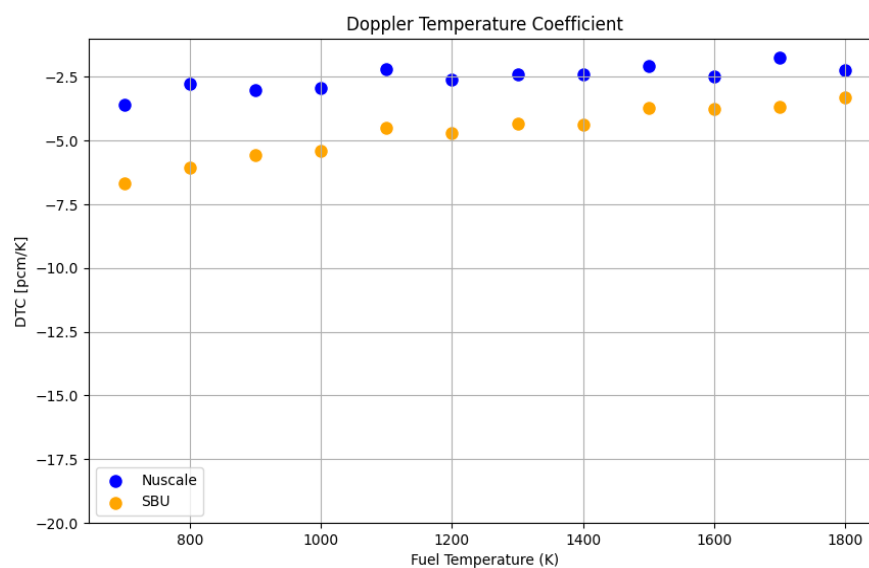
Figure 5 illustrates the Moderator Temperature Coefficient (MTC) in pcm/K as a function of moderator temperature. Both reactor cores show a negative MTC that increasing temperature decreases reactivity, thereby enhancing operational safety. The NuScale core (blue) keeps a nearly constant MTC up to 525 K, reflecting greater thermal stability. In contrast, the SBU core (orange) displays a more negative and variable MTC, suggesting higher sensitivity to temperature fluctuations and a greater need for precise control.

Figure 5: Moderator Reactivity Coefficient (MTC)



Furthermore, Figure 6 presents the Doppler Temperature Coefficient (DTC) for the NuScale and SBU reactors. Both reactors show a negative DTC, showing reduced reactivity with increasing fuel temperature. The conventional reactor shows a less negative DTC, reflecting lower sensitivity to temperature changes. In contrast, the SBU reactor has a more negative DTC, suggesting greater reactivity feedback, which can enhance thermal stability and safety but requires careful consideration alongside other operational parameters.

Figure 6: Comparative Doppler Temperature Coefficient (DTC).



Thus Figure 7 and Figure 8 presents three-dimensional graphs of linear power density (W/cm) across X and Y mesh coordinates. The NuScale core is a more uniform distribution of 126.7 W/cm, with a central peak and reduced risk of nucleate boiling, showing more stable operation. In contrast, the SBU core shows a higher power density of 225.6 W/cm with greater spatial variations, increasing the risk of overheating and needing stricter operational control. The average power density of the standard core is 18.47 kW/l, below the 46.5 kW/l recommended by the (International Atomic Energy Agency, 2024), while the SBU core provides 63% higher density but demands enhanced operational oversight.

Figure 7: Core NuScale Power Linear [W/cm].

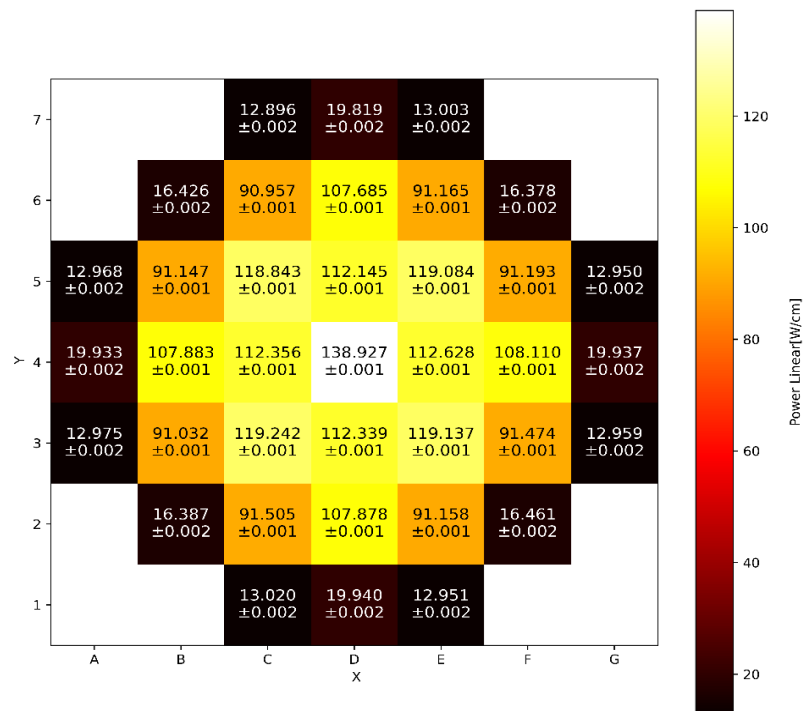
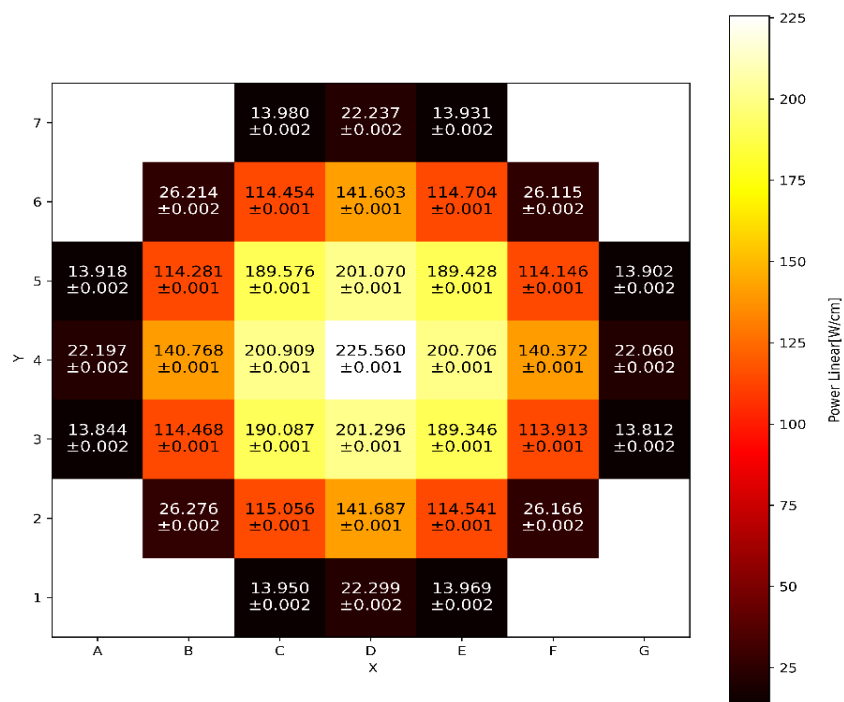
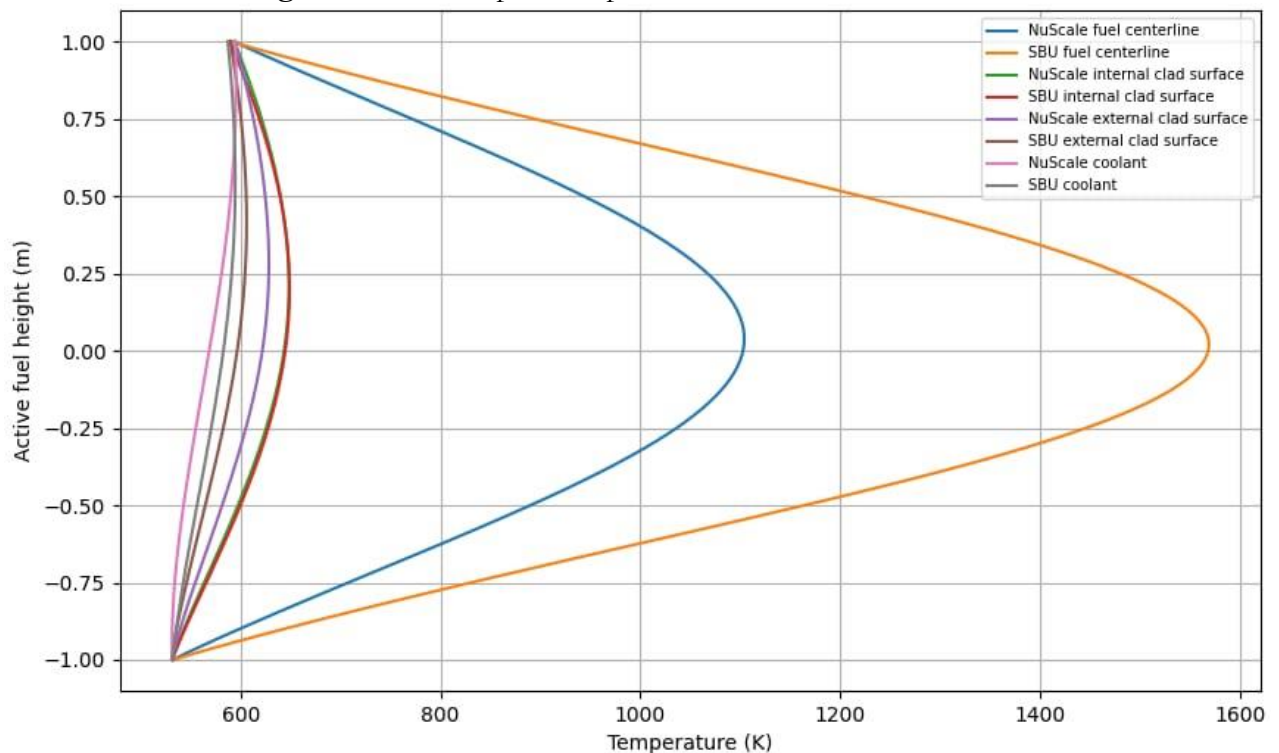


Figure 8: Core NuScale SBU Power Linear [W/cm].



The Computational Fluid Dynamics model shown maximum temperatures of 1104.25 K and 1569.49 K in the fuel pellet, and 648.37 K and 648.73 K in the cladding for the NuScale standard core and the SBU model, respectively. These values ensure that the fuel and core remain below the critical melting temperatures. Although the M5 material in the cladding has a lower heat transfer capacity compared to Zircaloy-4, as shown in (Kecek, et al., 2016), both designs-maintained temperatures within safe limits. Figure 9 shows the axial temperature distribution in the heated channel, highlighting the thermal behavior of the configuration.

Figure 9: Axial temperature profiles of NuScale and SBU cores.



The coolant flow channel is essential for reactor safety as it removes heat from the fuel rods. Considering only frictional and gravity losses, the pressure drops were 0.15492 bar and 0.06943 bar for the two cores. The CFD model showed average outlet temperatures of 589.64 K for the standard.

4. CONCLUSIONS

The comparison between the SBU and NuScale reactor cores highlights notable differences in reactivity control and performance. The original core features a more stable Boron Worth Coefficient (BWC) and better thermal stability, supporting safer and more predictable operation. In contrast, the SBU core exhibits greater sensitivity due to a more negative Doppler Temperature Coefficient (DTC), enhancing safety by providing stronger reactivity feedback at high temperatures.

NuScale demonstrates a more uniform and stable power density, favoring operational stability. Meanwhile, the SBU core offers improved fuel conversion efficiency and better performance under high-temperature conditions, though it requires more precise control and watching due to larger reactivity variations. Both designs stay within thermal safety limits; however, the SBU core may receive help from a more detailed thermohydraulic analysis to fully evaluate its performance under various operating conditions.

Computational Fluid Dynamics (CFD) simulations confirmed that maximum fuel pellet and cladding temperatures in both designs stay within safe limits for the materials used. Although the M5 alloy used in the fuel cladding has lower thermal conductivity than Zircaloy-4, thermal safety was adequately supported in both cores.

In summary, the choice between the two designs depends on specific operational requirements. The NuScale core offers greater stability and safety, making it suitable for standard operation. In contrast, the SBU core provides higher fuel efficiency and better high-temperature control but demands more rigorous management and detailed thermal-hydraulic evaluation.

FUNDING

The authors would like to acknowledge the funding and support of Brazilian research agencies: National Council for Scientific and Technological Development (CNPq), Coordination for the Improvement of Higher Education Personnel (CAPES) and Rio de Janeiro Research Support Foundation (FAPERJ), and the INCT for Innovative Reactors.

CONFLICT OF INTEREST

All authors declare that they have no conflicts of interest.

REFERENCES

- [1] AlRashidi, M. R. a. E.-H. M. E., 2009. A Survey of Particle Swarm Optimization Applications in Electric Power Systems. *IEEE Transactions on Evolutionary Computation*, pp. 913-918.
- [2] AlRashidi, M. R. A. M. F. E.-H. M. E. & E.-H. F., 2010. Applications of computational intelligence techniques for solving the revived optimal power flow problem. *Electric Power Systems Research*, pp. 694-702.
- [3] Andrew Johnson, D. K. S. T. a. G. R., 2020. serpentTools: A Python Package for Expediting Analysis with Serpent,. *Nuclear Science Engineering*.
- [4] Barthel, F. a. T. H., 2019. Thorium: Geology, Occurrence, Deposits and Resources.
- [5] Black, G., Shropshire, D. & Araújo, K., 2021. Small modular reactor (SMR) adoption: Opportunities and challenges for emerging markets. s.l.:Woodhead Publishing Series in Energy.
- [6] C.A.Lobo, M. & Stefani, G. L. d., 2024. Thorium as nuclear fuel in Brazil: 1951 to 2023. *Nuclear Engineering Design*.
- [7] Carelli, M. D. e. a., 2010. Economic Features of Integral, Modular, Small-to-Medium Size Reactors. *Nuclear Engineering and Design*, pp. 3267-3276.

- [8] Cunha, C. J. C. M. R. d. et al., 2024. Single heated channel analysis of the AP-Th 1000 concept. *Nuclear Engineering and Design*, Volume 420.
- [9] Galperin, A. S. M. & R. A., 1997. Thorium Fuel for Light Water Reactors – Reducing Proliferation Potential of Nuclear Power Fuel Cycle. *Science & Global Security*, pp. 265-290.
- [10] Ghimire, L. a. W. E., 2023. Small Modular Reactors: Opportunities and Challenges as Emerging Nuclear Technologies for Power Production. *Journal of Nuclear Engineering and Radiation Science*, p. 044501.
- [11] Gonçalves, D. M. E., Silva, M. V. d., Cunha, C. J. M. d. & Daniel Artur Pal, a., 2024. Feasibility of Converting NuScale SMRs from UO₂ to Mixed (Pu,Th)O₂ and (U,Th)O₂ Cores: A Parametric Study of the Seed-Blanket Fuel Assembly. *Nuclear Engineering and Design*, Volume 424.
- [12] Hussein, E. M., 2020. Emerging small modular nuclear power reactors: A critical review. *Physics Open*, p. 100038.
- [13] Hussein, E. M., 2020. Emerging small modular nuclear power reactors: A critical review. *Physics Open*.
- [14] IAPWS, 2008. IAPWS Industrial Formulation 1997 for the Thermodynamic Properties of Water and Steam. *International Steam Tables: Properties of Water and Steam Based on the Industrial Formulation IAPWS-IF97*, pp. 7-150.
- [15] Ingersoll, D., 2014. Deliberately small reactors and the second nuclear era. *Progress in Nuclear Energy*, pp. 128-135.
- [16] Ingersoll, M. D. C. & D. T., 2021. *Handbook of Small Modular Nuclear Reactors*. s.l.:Woodhead Publishing Series.
- [17] International Atomic Energy Agency, 2024. Advanced reactors information system (ARIS).. [Online] Available at: <https://aris.iaea.org/sites/power.html>
- [18] Jain, N. N. U. & J. J., 2018. A Review of Particle Swarm Optimization. *Eng. India Ser.* , pp. 407-411.
- [19] Jyothi, R. K., Melo, L. G. T. C. d., M.Santos, R. & Yoon, H.-S., 2023. An overview of thorium as a prospective natural resource for future energy. *Front. Energy Resources - Nuclear Energy*.

- [20] Kecek, A., Tucek, K., Holmstrom, S. & Uffelen, P. V., 2016. Development of M5 Cladding Material Correlations in the TRANSURANUS code. JRC Technical Reports, Issue 1, pp. 1-53.
- [21] Kennedy, J. & E. R., 1995. Particle swarm optimization. Proceedings of ICNN'95 - International Conference on Neural Networks, pp. 1942-1948.
- [22] Khorasani, S. & H. S., 2018. Control rod pattern optimization in nuclear reactors using PSO algorithm. Annals of Nuclear Energy, pp. 334-343.
- [23] Locatelli, G., Bingham, C. & Mancini, M., 2014. Small modular reactors: A comprehensive overview of their economics and strategic aspects. Progress in Nuclear Energy, pp. 75-85.
- [24] Luka Snoj, M. R., 2006. Calculation of Power Density with MCNP in TRIGA reactor. Nuclear Energy for New Europe.
- [25] NuScale Power, 2020. Part 2 - Final Safety Analysis Report (Rev.5)- Part 02 -Tier 02 - Chapter 04 - Reactor - Sections 04.01, s.l.: NuScale.
- [26] Pambudi, Y. D. S. a. W. W. a. K. B., 2016. Particle Swarm Optimization-Based Direct Inverse Control for Controlling the Power Level of the Indonesian Multipurpose Reactor. Science and Technology of Nuclear Installations, pp. 1-9.
- [27] Radkowsky, A. & G. A., 1998. The Nonproliferative Light Water Thorium Reactor: A New Approach to Light Water Reactor Core Technology. Nuclear Technology, pp. 215-222.
- [28] Radkowsky, A. & G. A., 2000. Thorium Fuel for Light Water Reactors: Reducing Proliferation Potential of Nuclear Power Fuel Cycle. Nuclear Technology, pp. 215-222.
- [29] Radkowsky, A., 1985. The Seed-Blanket Core Concept. Nuclear Science and Engineering, pp. 381-387.
- [30] Rosner, R. & S, G., 2011. Small Modular Reactors–Key to Future Nuclear Power Generation in the US. Energy policy institute at Chicago.
- [31] Silva, M. V. et al., 2024. Optimized modular nuclear reactor project utilizing artificial intelligence: Seed-blanket concept. Nuclear Engineering and Design.
- [32] Singh, A. K. & L. D. K., 2012. A hybrid PSO-GSA algorithm for optimization of control rod patterns in nuclear reactors. Annals of Nuclear Energy, pp. 220-230.

- [33] Stefani, G. L. d. et al., 2023. Feasibility to convert the NuScale SMR from UO₂ to a mixed (U,Th)O₂ core: Parametric study of fuel element - Seed-blanket concept. World Journal of Nuclear Science and Technology.
- [34] Todreas, N. E. & Kazimi, M., 2011. Nuclear Systems I -Thermohydraulic fundamentals. s.l.:Taylor & Francis.
- [35] Tong, G., Zhang, S., Wang, W. & Yang, G., 2023. A particle swarm optimization routing scheme for wireless sensor networks. Transactions on Pervasive Computing and Interaction.
- [36] Valtavirta, E. F. a. Y. B. a. V., 2023. Definition of the neutronics benchmark of the NuScale-like core. Nuclear Engineering and Technology, pp. 3639-3647.
- [37] Westinghouse, 2011. AP1000 Design Control Document Rev. 19. , ML11171A500, 2011, s.l.: U.S. Nuclear Regulatory Commission.
- [38] Xu, Q. a. W. T. a. W. W., 2021. Nonlinear Dissipative Particle Swarm Algorithm and Its Applications. IEEE Access, pp. 158862-158871.
- [39] Xu, Y. J. S. W. G. & L. Z., 2021. Nonlinear dissipative particle swarm optimization algorithm for nuclear reactor core design. Annals of Nuclear Energy, p. 108124.
- [40] Yang, X.-F. X. a. W.-J. Z. a. Z.-L., 2002. Dissipative particle swarm optimization. Proceedings of the 2002 Congress on Evolutionary Computation. CEC'02 (Cat. No.02TH8600), pp. 1456-1461.

LICENSE

This article is licensed under a Creative Commons Attribution 4.0 International License, which permits use, sharing, adaptation, distribution and reproduction in any medium or format, as long as you give appropriate credit to the original author(s) and the source, provide a link to the Creative Commons license, and indicate if changes were made. The images or other third-party material in this article are included in the article's Creative Commons license, unless indicated otherwise in a credit line to the material.

To view a copy of this license, visit <http://creativecommons.org/licenses/by/4.0/>.